Human Molecular Genetics, 2012, Vol. 21, No. 26 ***5511–5527***
doi:10.1093/hmg/dds395
Advance Access published on September 21, 2012

A novel role for doublecortin and doublecortin-like kinase in regulating growth cone microtubules

Daphney C. Jean[1], Peter W. Baas[1,†] and Mark M. Black[2,*,†]

[1]Department of Neurobiology and Anatomy, Drexel University College of Medicine, 2900 Queen Lane, Philadelphia, PA 19129, USA [2]Department of Anatomy and Cell Biology, Temple University School of Medicine, 3420 North Broad Street, Philadelphia, PA 19140, USA

Received July 11, 2012; Revised and Accepted September 14, 2012

Doublecortin (DCX) and doublecortin-like kinase (DCLK), closely related family members, are microtubule-associated proteins with overlapping functions in both neuronal migration and axonal outgrowth. In growing axons, these proteins appear to have their primary functions in the growth cone. Here, we used siRNA to deplete these proteins from cultured rat sympathetic neurons. Normally, microtubules in the growth cone exhibit a gently curved contour as they extend from the base of the cone toward its periphery. However, following depletion of DCX and DCLK, microtubules throughout the growth cone become much more curvy, with many microtubules exhibiting multiple prominent bends over relatively short distances, creating a configuration that we termed wave-like folds. Microtubules with these folds appeared as if they were buckling in response to powerful forces. Indeed, inhibition of myosin-II, which generates forces on the actin cytoskeleton to push microtubules in the growth cone back toward the axonal shaft, significantly decreases the frequency of these wave-like folds. In addition, in the absence of DCX and DCLK, the depth of microtubule invasion into filopodia is reduced compared with controls, and at a functional level, growth cone responses to substrate guidance cues are altered. Conversely, overexpression of DCX results in microtubules that are straighter than usual, suggesting that higher levels of these proteins can enable an even greater resistance to folding. These findings support a role for DCX and DCLK in enabling microtubules to overcome retrograde actin-based forces, thereby facilitating the ability of the growth cone to carry out its crucial path-finding functions.

INTRODUCTION

Doublecortin (DCX) is a microtubule-associated protein first identified as a gene product associated with the neuronal migration disorder known as lissencephaly (1). Pathological mutations in DCX impair its binding to microtubules (2), indicating that the loss of microtubule functions dependent on DCX underlies lissencephaly. Initial mouse models exploring the underlying mechanisms of lissencephaly revealed limited migratory phenotypes due to genetically redundant pathways that compensate for the lack of DCX. DCX is a member of a larger gene family that includes doublecortin-like kinase 1 (DCLK). Depleting both DCX and DCLK produces a more severe phenotype than depleting either protein alone (3,4). Furthermore, double knockdowns display widespread axonal defects in mice, and this is also the case when cortical or hippocampal neurons from these animals are grown in culture (3,4).

Clues about the potential functions of DCX and DCLK are suggested by their distribution in growing axons. We recently confirmed earlier observations that DCX is enriched in the growth cones of elongating axons (5–7), and further showed that DCX associates in a gradient along microtubules that increase sharply as they extend from the base of the growth cone to its periphery (8). DCLK exhibits a similar distribution, suggesting that both proteins specialize microtubules for the unique environment of the growth cone compared with the axonal shaft (9).

Growth cones can be divided into three regions (10). The peripheral domain is the flattened actin-rich lamellar part of the cone, which also includes its filopodia. The central domain is contiguous with the axonal shaft and contains the

*To whom correspondence should be addressed. Tel: +1 2157073165; Fax: +1 2157072966; Email: mark.black@temple.edu
†These co-senior authors contributed equally.

majority of the microtubule mass of the growth cone. The transition zone lies at the interface of these two domains; it is a gateway through which microtubules must pass in order to enter the peripheral domain from the central domain. Such entry is essential for sustained axonal growth, and the spatial polarization of such entry is necessary for growth cone turning (10). A potential role for DCX and DCLK in the entry of microtubules into the peripheral domain is suggested not only by the enrichment of these proteins on distal regions of microtubules but also by findings that DCX can interact with actin filaments and may contribute to interactions between actin filaments and microtubules (11,12). Another possibility is that DCX and DCLK may directly impact properties of microtubules that influence their ability to invade the peripheral domain. Cryo-electron microscopy has revealed that DCX binds between the protofilaments of microtubules (13), which may be conducive to enabling the microtubule to remain relatively straight. A molecular mechanism to limit microtubule curvature might be especially important in growth cones, where microtubules are subjected to forces generated by various molecular motor proteins. Our present goal was to pursue this idea.

RESULTS

Here, we used a combination of acute knockdown and overexpression approaches on cultured rat sympathetic neurons to explore the impact of DCX and DCLK on the properties of microtubules in growth cones and on growth cone navigation behaviors. In our previous studies, no obvious phenotypes were observed when DCX alone was depleted from these neurons (8); axons grew at normal rates and the growth cones of DCX-depleted neurons were not noticeably different from controls in terms of morphology or microtubule distribution. These findings are consistent with the results of other studies in which targeted deletion of DCX in mice produced relatively mild phenotypes (3,14). Similarly, targeting of DCLK, a closely related family member, also produced a mild phenotype (3). However, targeting of both DCX and DCLK produced a more dramatic phenotype with significant impairment in axonal growth (3,4). These findings suggest that DCX and DCLK have at least partially redundant functions and that one can largely compensate for the other in single knockdown experiments. When both proteins are depleted, the loss of their combined contributions to axonal growth becomes readily apparent. Thus, in the present studies, we have targeted both DCX and DCLK together, rather than further exploring the impact of depleting either one of them on its own.

DCLK is preferentially concentrated on growth cone microtubules

As shown in Figure 1, DCLK is highly enriched in the neuronal growth cone compared with the axonal shaft, confirming previous results of Burgess and Reiner (9). Figure 1 also shows that DCLK localizes to microtubules in the growth cone and its relative abundance on these microtubules increases progressively as microtubules extend from the base of the cone toward its tip. Thus, DCLK closely resembles DCX (8) in terms of its localization and microtubule association in growth cones of cultured sympathetic neurons.

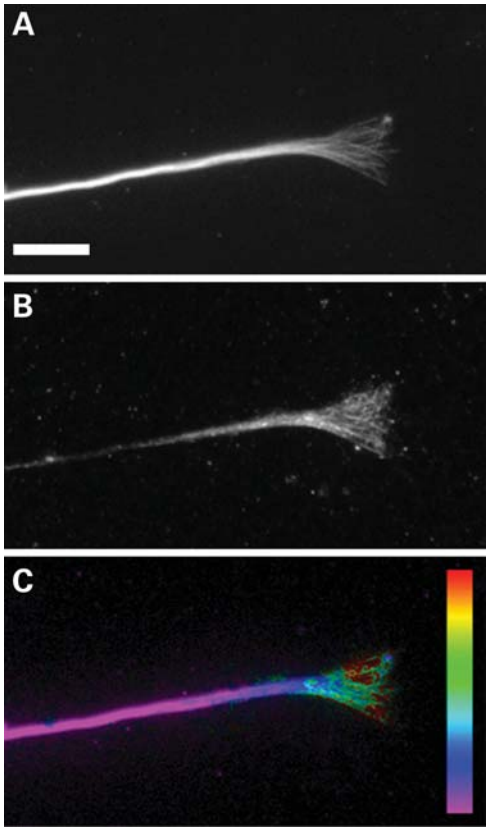

Figure 1. DCLK is enriched in the growth cone. Immunofluorescence staining of tubulin (**A**) and DCLK (**B**) in a growth cone and distal region of an axon of a rat sympathetic neuron in culture. (**C**) Ratio-image depicting the abundance of DCLK relative to microtubules. Note that the enrichment of DCLK on microtubules increases in a proximal-to-distal manner from the base of the growth cone toward the peripheral domain, reaching the highest concentration on microtubules that extend into the peripheral domain. Scale bar = 8 μm.

Double knockdown of DCX and DCLK impairs axonal growth

To co-deplete DCX and DCLK, siRNA SMARTpools targeting each of them were introduced simultaneously by nucleofection into neurons just prior to plating. The neurons were then cultured for 3 days, which is sufficient time to allow for the near complete depletion of the proteins [based on our previous work on DCX (8) and microtubule motor proteins (15,16)], after which the neurons were re-plated and challenged to re-grow axons in the near absence of DCX and DCLK. Visual inspection of immunostained samples revealed that both DCX and DCLK levels were reduced in all neurons, with the majority of neurons failing to stain above background levels (background was determined by staining control neurons using non-immune antibodies in place of the DCX or DCLK antibodies). Quantitative analyses showed that staining for DCX was reduced to background levels in 90% of the neurons; while that of DCLK was reduced to background

Table 1. Effects of depletion of DCX+DCLK on neuronal morphology

	Axons/ cell	Axon length, mean ± SD	Branches/ axon
Control neurons	1.8 ± 0.97	157 ± 39	3.1 ± 1.8
DCX+DCLK-depleted neurons	2.5 ± 1.7	139 ± 57	2.5 ± 1.7
P (*t*-test)	≤0.006	≤0.03	0.05

Results from a representative experiment examining the indicated parameters of neuronal morphology. The data are based on analyses of 70 control neurons and 69 neurons depleted of both DCX and DCLK.

levels in 85% of the neurons (these numbers are based on assessing a total of 200 neurons in two representative cultures). The combined depletion of both DCX and DCLK resulted in a subtle axonal growth phenotype. By visual inspection, it was clear that depleted neurons had extended axons that were not obviously different from controls. However, quantitative analyses revealed that compared with controls, neurons depleted of both DCX and DCLK produced fewer axons per cell, and the axons were shorter and slightly more branched (Table 1).

Double knockdown of DCX and DCLK alters the contour of growth cone microtubules

In addition to the morphological effects of DCX and DCLK depletion on the neuron, there were also notable effects on the microtubules in the growth cone that were revealed by more detailed analyses. At first glance, the microtubule array in the growth cones of DCX+DCLK-depleted neurons appears more tangled than that of control neurons (Fig 2), and as a result, it is more difficult to trace individual polymers for any appreciable length. On closer inspection, this appears to be due to an increase in the curviness of microtubules in DCX+DCLK-depleted neurons. In control growth cones, microtubules commonly exhibit a gently curved contour as they extend from the growth cone base toward the periphery. By contrast, relatively few microtubules in the growth cone exhibit this gently curved contour in neurons depleted of DCX and DCLK. Instead, many have multiple bends along their length, giving them an undulated appearance (Figs 2 and 3). As a result, the microtubules throughout the growth cone appear to repeatedly cross over each other as they extend from its base toward the periphery. The net effect is a growth cone microtubule array that appears more highly intertwined than that of control neurons.

To quantify this phenotype, we took advantage of a feature common to many of these undulated microtubules, which is the presence of multiple bends along their length that causes them to fold into wave-like shapes (Fig. 3). We defined wave-like folds as consisting of a series of at least four bends occurring within a distance of 5 μm or less, with the bends creating segments of at least 0.5 μm in length. These criteria selected specifically for microtubules with prominent folds that occurred over relatively short distances along their length, and excluded microtubules that had fewer bends or in which the bends were more spread out along the length of the polymer (Fig. 3). In addition, we also focused only on microtubules that could be unambiguously traced for at least 5 μm to their distal ends. While this limited the number of microtubules that were evaluated for these analyses, it ensured that single discrete microtubules were analyzed for the presence of wave-like folds. Figure 3 shows several examples of microtubules that satisfy these criteria as well as several with bends that do not satisfy these criteria. Quantitative analyses (Fig. 4) showed an approximate doubling in the proportion of microtubules with wave-like folds as a result of depletion of DCX and DCLK, increasing from 15.6 to 27.5% ($P \leq 0.0001$ χ^2-test). Thus, while microtubules with wave-like folds are present in control growth cones, their frequency increases significantly as a result of depletion of DCX and DCLK.

In the course of these studies, we compared the frequency of wave-like folds in control and DCX+DCLK-depleted neurons as part of three separate experiments, and the results are shown in Table 2. All of these analyses were performed on fixed cells using the criteria specified above (see also Materials and Methods) to score growth cone microtubules as positive or negative for wave-like folds. As can be seen, there is some variability in the frequencies determined from one experiment to the next. The basis for this is uncertain. One possibility is that it may relate to variations in axonal growth behavior from one set of cultures to another. However, we consider this unlikely because in our experience, rat sympathetic neurons are generally consistent in their growth behavior using the culture conditions described in the present studies. In particular, we studied neurons under conditions of laminin-stimulated axonal growth during which the axons undergo relatively steady elongation at rates of ~22 μm/h, and a few axons are observed to undergo more than momentary pauses in their growth (17–19). While the basis for the variation in frequency of microtubules with wave-like folds remains unknown, we note that depleting DCX and DCLK consistently results in an approximate doubling of this frequency, a result that is statistically highly significant in each experiment. This gives us confidence that the criteria used for scoring microtubules with wave-like folds allow us to reliably evaluate whether specific experimental manipulations alter this parameter.

We used live-cell imaging approaches to obtain an independent measure of the frequency of microtubules with wave-like folds in control and DCX+DCLK-depleted neurons. Microtubules were labeled for live-cell imaging using EGFP-EB3. EB3 is a tip-binding protein that associates with microtubule plus ends during assembly (20). In time-lapse movies, EGFP-EB3 appears as a moving 'comet' at the plus end of growing microtubules because of the steady addition of new EGFP-EB3 molecules at the growing tip combined with the gradual dissociation of previously added EB3 molecules behind the microtubule tip. While EB3 binds preferentially at the tip of growing microtubules, low amounts associate with the polymer behind the tips and this can be revealed by enhancement of the images. We used time-lapse imaging of EGFP-EB3 to evaluate the effects of DCX+DCLK depletion on the wavy contour of growing microtubules in the peripheral domain of the growth cone.

cDNA for EGFP-EB3 was nucleofected into neurons along with appropriate siRNAs, the cells were cultured for 3 days to deplete DCX and DCLK and then re-plated as described in

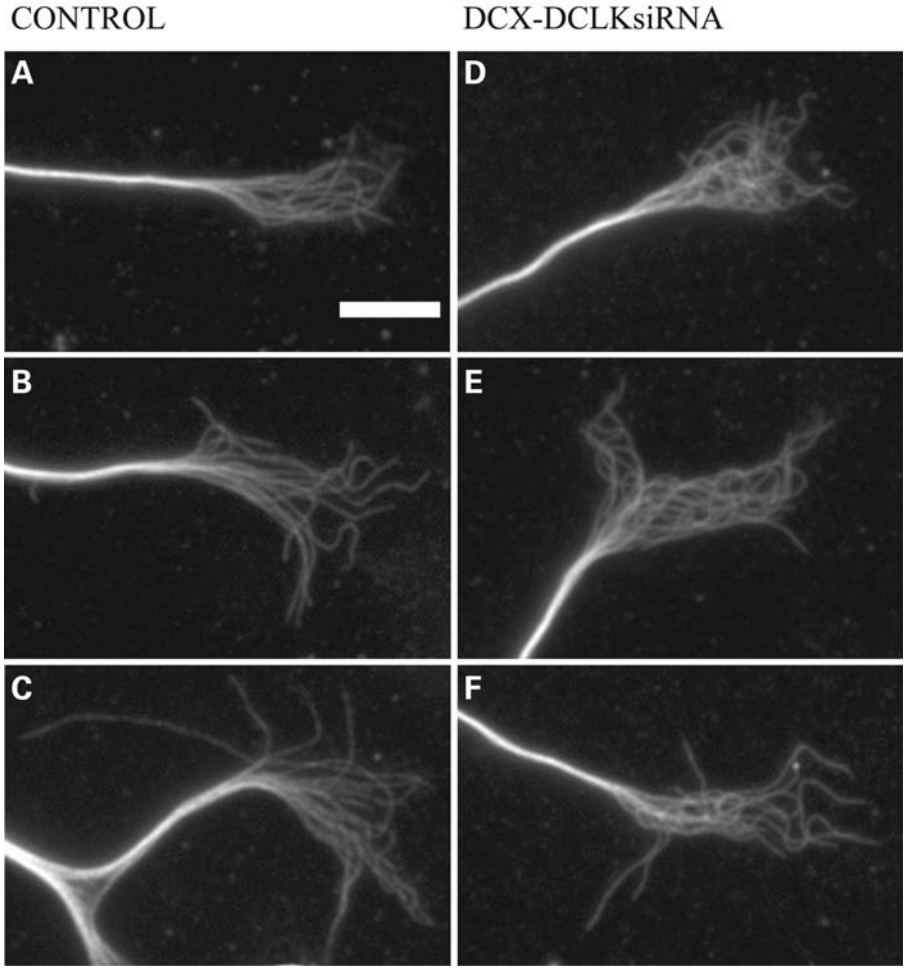

Figure 2. siRNA-mediated depletion of DCX and DCLK results in enhanced tangling of growth cone microtubules. (**A**–**C**) Immunofluorescence staining of tubulin in three control growth cones. Growth cone microtubules of control neurons typically exhibit a curvy contour, and many can be traced from the central into the peripheral domain. (**D**–**F**) Three growth cones of neurons treated with siRNA SMARTpools to DCX and DCLK. Overall the appearance of the microtubule array in the growth cone is notably more tangled than in control growth cones. Scale bar = 6 μm.

Materials and Methods. Live-cell imaging was then performed to evaluate the curviness of microtubules in the growth cone. As with the fixed cell analyses, the microtubule array in growth cones of depleted neurons appeared more tangled than in control neurons (Fig. 5). In addition, microtubules with wave-like folds in the peripheral domain of the growth cone were readily apparent in the live-cell imaging analyses of growth cones of both control and DCX+DCLK-depleted neurons (single arrowheads in Fig. 5A and B). These analyses revealed that the trajectory of the EB3 comets was relatively straight with wave-like folds occurring at variable distances behind the comets, as if the microtubules were growing, but also encountering forces that caused the polymer to buckle behind its tip. We quantified the frequency of microtubules with wave-like folds in the peripheral domain of the growth cones of control neurons and neurons depleted of both DCX and DCLK using the same criteria as in our fixed cells analysis. These live-cell analyses revealed a higher frequency of microtubules with wave-like folds in control neurons (30%) compared with analyses based on fixed cells (8.6–15.6%, Table 1). Depletion of DCX and DCLK increased the percentage of microtubules with wave-like folds to ~70%, an increase that is statistically highly significant ($P < 0.0001$, χ^2-test).

The basis for the differences in the relative abundance of microtubules with wave-like folds detected using fixed cell versus live-cell imaging approaches is uncertain. Such differences may reflect the fact that the live-cell images are simpler with less microtubule overlap, permitting evaluation of more of the polymers. It is also possible that it relates to the fact that the use of EGFP-EB3 in live-cell imaging specifically highlights growing microtubules, and that the percentage of microtubules with wave-like folds is higher among growing microtubules compared with the total population of microtubules. Regardless, both types of analyses reveal that the combined depletion of DCX and DCLK results in a significant increase in the percentage of microtubules in the growth cone that exhibit wave-like folds along their length.

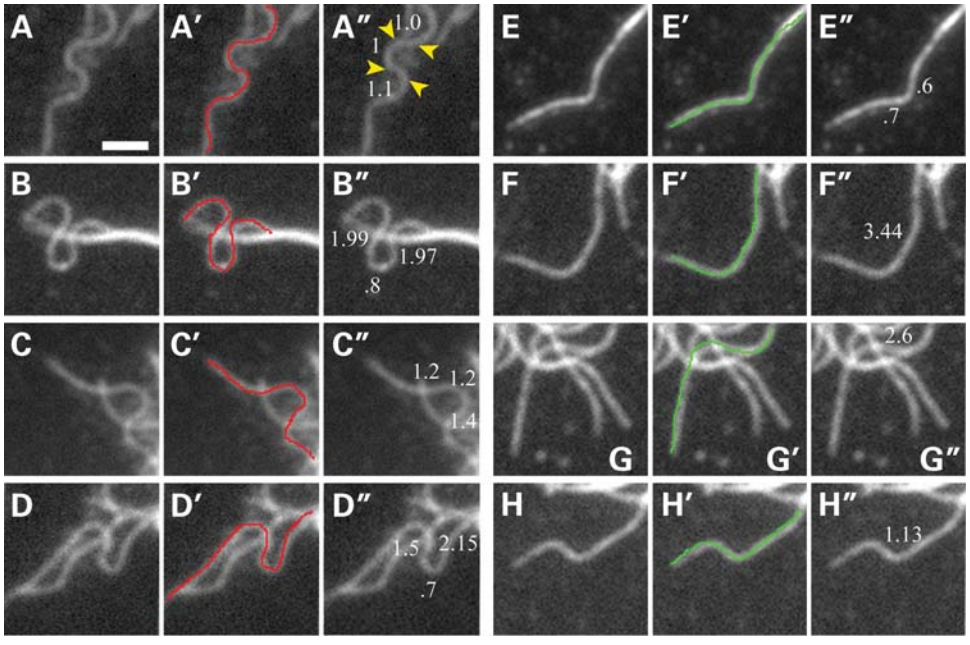

Figure 3. Characterization of microtubules with wave-like folds. The figure shows four examples of microtubules that meet the criteria of wave-like folds (see Materials and Methods for details) (**A**–**D**) and four microtubules with bends but that do not satisfy the criteria for wave-like folds (panels **E**–**H**). The first, second and third panels of each set, respectively, show the microtubule image, a traced line over the microtubule of interest and the length (in microns) of the segments formed by the bends. Microtubules were categorized as having wave-like folds if the microtubule contained four consecutive bends within a maximum distance of 5 μm. The microtubules highlighted in (A)–(D) meet this criteria; the yellow arrowheads in (A″) identify the approximate positions of the four bends that comprise one of the folds apparent on this microtubule. In any given control or depleted growth cone, many microtubules exhibited bends but did not satisfy the criteria for wave-like folds; these latter microtubules typically had too few bends or the bends were more spaced along the length of the polymer (E–H). Scale bar = 1.8 μm.

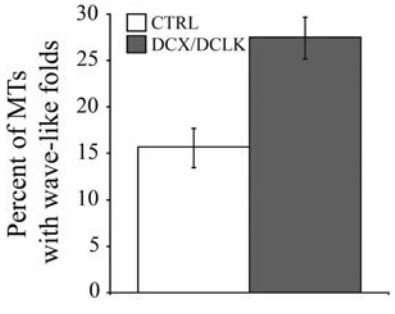

Figure 4. Quantitative analyses showing the effect of DCX–DCLK depletion on the contour of growth cone microtubules. The graph shows the percentage of microtubules with wave-like folds in growth cones of control neurons and neurons depleted of DCX+DCLK. Knockdown of both DCX and DCLK significantly increased the frequency of microtubules with wave-like folds [$P < 0.0001$, χ^2-test, comparing control neurons (90 growth cones) with depleted neurons (92 growth cones)].

Table 2. Effects of depletion of DCX and DCLK on the frequency of growth cone microtubules with wave-like folds

Experiment #	Frequency of wave-like folds mean ± SD (# growth cones)		
	Control	DCX + DCLK-depleted	Chi^2 *P*-value
1	15.6 ± 19.4% (90)	27.5 ± 21% (92)	≤0.0001
2	8.6 ± 9.2% (57)	15.4 ± 8.5% (57)	≤0.02
3	12 ± 12.0% (73)	26 ± 15.4% (53)	≤0.0001

The percentage of microtubules with wave-like folds in three independent experiments. While there is variability in the percentage of microtubules with wave-like folds between experiments, we consistently found an ∼2-fold increase in the percentage in DCX- and DCLK-depleted neurons compared with control, and all differences within individual experiments were statistically significant.

The regions of microtubules with wave-like folds in control growth cones are deficient in DCX

Given that microtubules with wave-like folds are present in control growth cones and that depleting DCX and DCLK significantly increases the number of microtubules with this feature, we sought to determine whether microtubules with wave-like folds in control growth cones are normally deficient in DCX. Figure 6 shows two growth cones of control cells double stained for microtubules and DCX. Each growth cone contains one microtubule with a wave-like fold, and these stain much less consistently along their length than the relatively straight microtubules in the same growth cones. The wave-like folds typically exhibit a few discrete punctae of staining that are relatively widely spaced along the curved part of the polymer. By contrast, relatively straight segments of microtubules show much more continuous staining along their length. Visual inspection also reveals other microtubules with discrete segments that stain relatively poorly for DCX. While these latter microtubules do not satisfy the criteria established for having wave-like folds, the regions deficient in DCX staining in most cases exhibit prominent curvature (Fig. 8D–F). These results indicate that the amount of DCX associated with a microtubule varies along its length depending on the degree of curvature. For straight

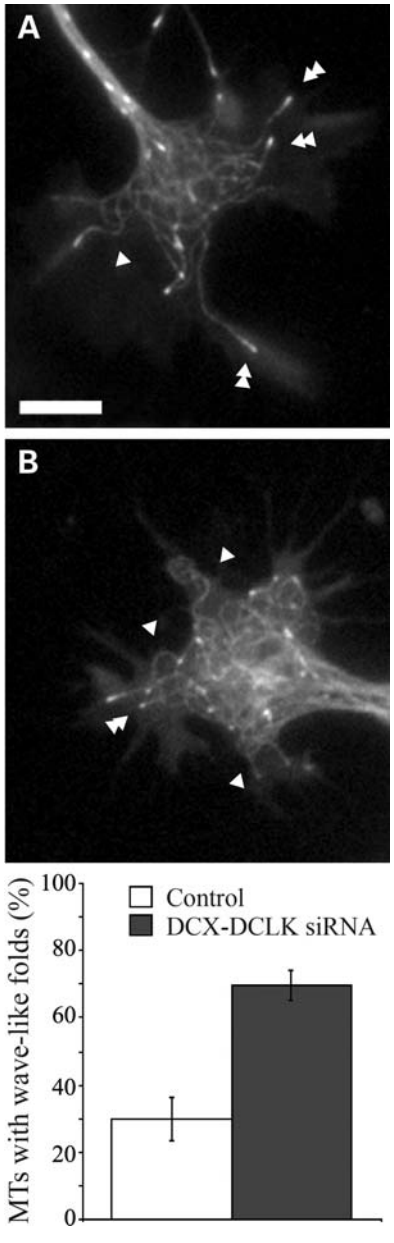

Figure 5. Microtubules tangling in growth cones of living neurons. (**A**) and (**B**) show growth cones in single frames from time-lapse sequences of EGFP-EB3 from a control (A) or DCX+DCLK-depleted neuron (B). Scale bar = 3 μm. Note the difficulty in tracing individual microtubules in the growth cone of the depleted neuron compared with the control. This is a manifestation of the enhanced tangling of growth cone microtubules as a result of depletion of DCX+DCLK. Microtubules with wave-like folds (single arrowheads) were more apparent in growth cones of DCX+DCLK-depleted neurons compared with controls, an impression confirmed by quantitative analysis (see graph), which revealed more than a 2-fold increase in the frequency of microtubules with wave-like folds in DCX−DCLK depleted neurons compared with control ($P < 0.0001$, χ^2-test). Double-arrowheads denote microtubules without wave-like folds MTs, microtubules.

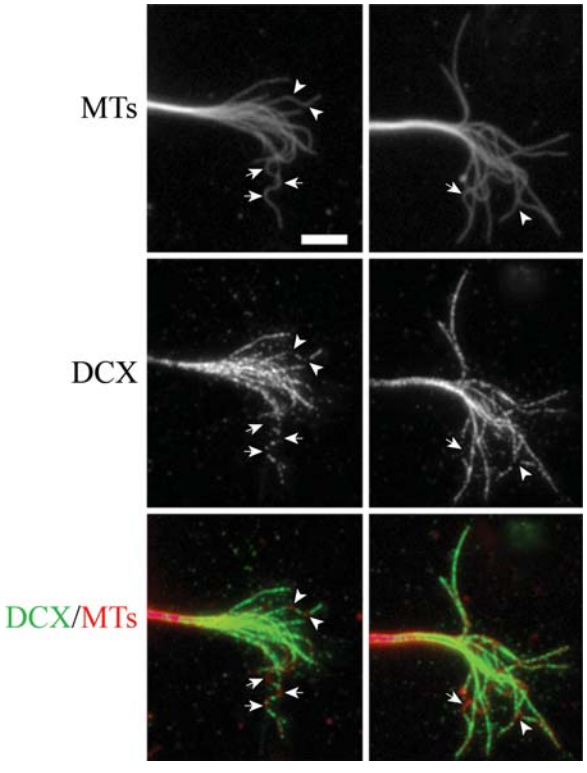

Figure 6. Highly curved segments of microtubules in control growth cones are deficient in DCX. Here, we show the immunofluorescence staining of microtubules (upper panels) and DCX (middle panels) in the growth cone of two control neurons. Arrows identify segments of microtubules with wave-like folding, whereas arrowheads identify bends along microtubules that do not meet the criteria of having wavelike folds. (**C**) A color overlay of these images with microtubules in red and DCX in green. Note the lack of DCX on the regions of the microtubules that are highly curved. Scale bar = 6 μm MTs, microtubules.

or gently curving polymers, the association appears fairly regular along their length. However, DCX is deficient at regions along the length of microtubules with prominent bends. This is particularly striking in wave-like folds because they consist of multiple bends occurring over relatively short lengths of the polymer. We tried to determine whether DCLK is also deficient on curvilinear segments of microtubules. However, the antibody to DCLK did not produce images of sufficient quality to unequivocally assess this issue.

Overexpression of DCX straightens growth cone microtubules

The previous section documents that depleting DCX and DCLK enhances the frequency of microtubules with prominent curvature. This raises the possibility that these proteins regulate properties of microtubules that impact their relative straightness. If this is correct, then a reasonable expectation is that overexpression of DCX should increase the frequency of straight microtubules in the peripheral domain at the expense of microtubules with wave-like folds, and in addition may rescue the phenotype of neurons depleted of DCX and DCLK. We have directly tested these predictions by expressing human DCX, coupled to EGFP, in control and DCX+-DCLK-depleted neurons. Even though the sequence for human DCX is ∼90% similar to that of rat DCX, co-nucleofection of the EGFP-DCX cDNA with the DCX and DCLK siRNAs resulted in significant overexpression of DCX. This may relate to the sequence difference between

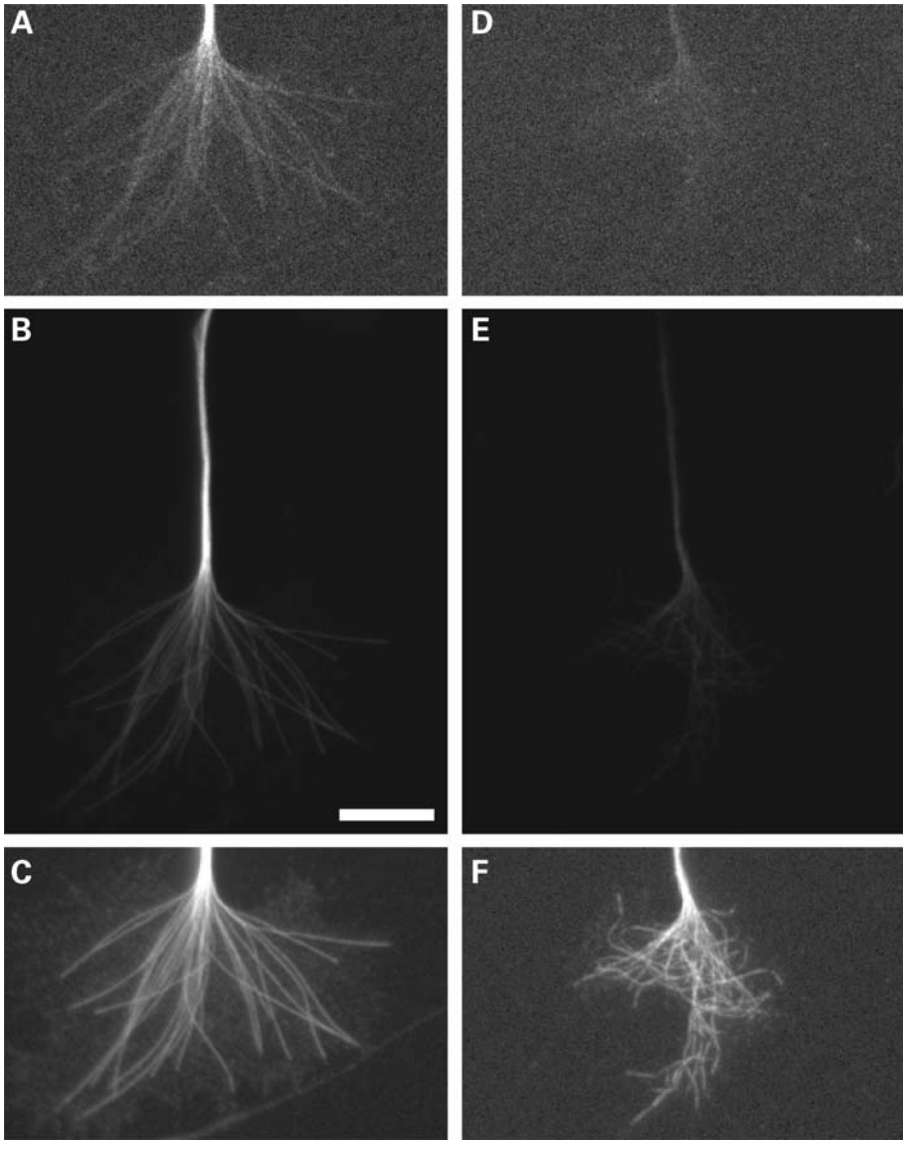

Figure 7. DCX overexpression straightens growth cone microtubules. Left and right panels are images of two representative control growth cones from a culture of transfected neurons, one that highly expressed EGFP-DCX (**A**–**C**), and one that minimally expressed this construct (**D**–**F**). (A and D) Staining for EGFP to demonstrate the relative level of expression. (B and E) Staining for DCX in which the exposure times and enhancing are identical. Visual inspection provides an indication of the relative abundance of DCX in the two neurons, and it is clear that the abundance of DCX is several-fold greater in the neuron expressing exogenous DCX (B) compared with the cell that is not expressing ectopic DCX (E). Quantitative analyses indicate that on average, neurons expressing the human DCX contained ∼6-fold more DCX in the growth cone than neurons that did not express the human DCX. (C and F) The same growth cones depicted in (B) and (E), but each enhanced differently to optimize visualization of growth cone microtubules staining for DCX; microtubules are strikingly straighter in the neuron overexpressing DCX. Scale bar = 6 μm.

human and rat or to the level of the ectopic expression simply overwhelming the levels of siRNA in the cells. In both control cells and siRNA-treated cells, transfection with the EGFP-DCX cDNA was fairly efficient, with ∼40% of the neurons expressing readily detectable amounts of EGFP-DCX. For the present purposes, we selected for analyses neurons that extended normal appearing axons with typical looking growth cones. Figure 7 shows DCX staining of two representative control growth cones from a culture of transfected neurons, but only one of which exhibited detectable expression of EGFP-DCX. The DCX staining of the expressing cell is much more intense than that of the non-expressing cell (compare Fig. 7B and E). To estimate the increased expression, we compared DCX staining intensity of growth cones of non-expressers with that of overexpressers. For non-expressers, the mean intensity was 4.5E5 ± 2.03E5 (mean ± SD, range of 1E5–7E5, $n = 8$ growth cones), whereas for overexpressers, the mean intensity was 2.7E6 ± 1.99E6 (range of 8E5–8E6, $n = 12$) for an average of a 6-fold increase in DCX expression. We also note that in cells highly expressing EGFP-DCX, DCX staining in the growth cone is clearly filamentous and in a pattern indicative

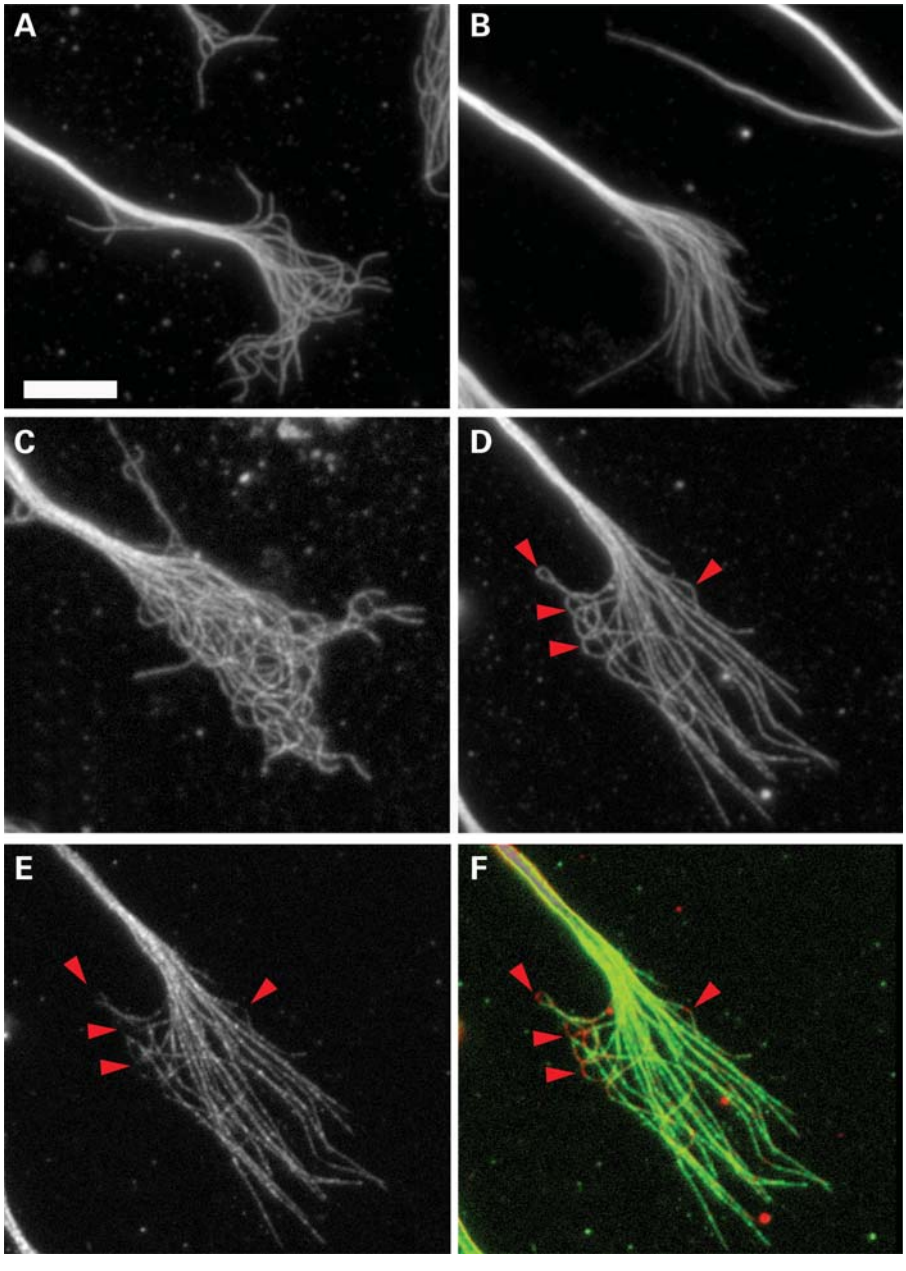

Figure 8. Overexpression of DCX straightens growth cone microtubule. (**A** and **B**) Growth cones of control siRNA neurons transfected with cDNA encoding EGFP or EGFP-DCX cDNA. Overexpression of the EGFP-DCX causes the microtubules to become straighter and significantly decreases the percentage of microtubules with wave-like folds. (**C** and **D**) Growth cones of DCX+DCLK siRNA-treated neurons that were co-transfected with cDNAs to EGFP or human DCX tagged with EGFP. The knock-in of the human DCX in the neurons treated with DCX+DCLK siRNA also resulted in straightening of growth cone microtubules and thereby largely reversing the tangling and wave-like folding phenotypes caused by depletion of DCX+DCLK. (**E**) The GFP staining of the DCX+DCLK siRNA-treated neuron shown in (D). (**F**) A color overlay of (D) and (E) with microtubules in red and GFP in green. Note the lack of EGFP (red arrowhead) on the regions of the microtubule with prominent bends. Scale bar = 6 μm.

of association with microtubules. Thus, in the overexpressers not only is there more DCX, there is also relatively more DCX on the microtubules in the growth cone.

Overexpression of DCX rendered microtubules throughout the growth cone of control cells straighter compared with microtubules in cells with just endogenous amounts of DCX (Fig. 7C and F), and dramatically reduced the number of microtubules with wave-like folds (Figs 7 and 8). Under the conditions of these experiments, there was no indication that overexpression of DCX induced the formation of microtubule bundles in the growth cone (Figs 7 and 8). Thus, the effect of DCX overexpression on the conformation of microtubules was not secondary to microtubule bundling. Furthermore, overexpression of human DCX reversed the effects of depleting endogenous DCX and DCLK on the appearance of microtubule tangling in the growth cone, with the vast majority of

growth cone microtubules appearing relatively straight (Fig. 8C and D). Overexpression of DCX significantly reduced the percentage of microtubules with wave-like folds in control neurons and in neurons treated with DCX+DCLK siRNA. Using the criteria described above for quantifying wave-like folds, the frequency of assessed microtubules with wave-like folds in control neurons decreased from 8.6 ± 9.2% (mean ± SD, $n = 57$ growth cones) to 3.2 ± 4.1% ($n = 48$) with overexpression of EGFP-DCX ($P \leq 0.05$, χ^2-test). Co-transfection of EGFP-DCX with DCX+DCLK siRNA more than reversed the increase in frequency of microtubules with wave-folds normally caused by depletion of DCX and DCLK so that the frequency was comparable with that seen in control neurons overexpressing human DCX [15.4 ± 8.5% (mean ± SD, $n = 57$ growth cones treated with DCX+DCLK siRNA) versus 3.8 ± 5.7% ($n = 51$ growth cones treated with DCX+DCLK siRNA and expressing EGFP-DCX) $P \leq 0.001$, χ^2-test]. We also note that when microtubules with highly curvilinear segments were encountered in cells overexpressing the human DCX, these curvilinear segments were relatively deficient in EGFP-DCX, whereas the straight portions of the microtubules were enriched in EGFP_DCX (Fig. 8D–F), providing further evidence that DCX is deficient on segments of microtubules with prominent bends.

Depletion of MAP1B does not enhance the presence of wave-like folds along growth cone microtubules

Several microtubule-associated proteins in addition to DCX and DCLK are present on growth cone microtubules, among which MAP1B is particularly abundant. MAP1B is present on microtubules throughout the axon as well as the growth cone, and in the growth cone its distribution largely overlaps with that of DCX and DCLK. Although MAP1B does show a marked enrichment on microtubules in the distal region of the axon, it does not show the prominent gradient characteristic of DCX and DCLK (21). To ascertain whether depleting MAP1B also impacts the frequency of microtubules with wave-like folds in the growth cone, we depleted MAP1B using siRNA. In our hands, 3 days after introducing the siRNA into dissociated sympathetic neurons, 90% of the neurons showed no detectable immunostaining for MAP1B (data not shown; 22). When re-plated after depletion of MAP1B, the neurons extended normal appearing axons, although the axons were shorter than control neurons, as previously described (23,24). By visual inspection, the microtubule array in growth cones of MAP1B-depleted neurons was not notably different from that of control neurons, and did not have the highly tangled appearance typical of that seen in neurons depleted of both DCX and DCLK. The frequency of microtubules with wave-like folds in the peripheral domain of MAP1B-depleted neurons was indistinguishable from that of control neurons [8.5 ± 7.3% ($n = 57$ growth cones) versus 7.9 ± 8% ($n = 60$ growth cones), respectively, $P > 0.1$, χ^2-test]. Thus, the enhanced microtubule bending caused by depleting DCX and DCLK is not a general response to depleting any microtubule-associated protein.

Inhibition of the myosin-II-powered retrograde flow of actin straightens growth cone microtubules

One potential explanation for the wavy contour of growth cone microtubules is that they are buckling in response to forces imposed upon them either directly or indirectly by molecular motors. In this regard, retrograde flow of actin filaments imposes a force on growth cone microtubules that can push them back toward the axonal shaft (25–27). This is believed to be the reason why the peripheral domain has relatively little microtubule mass, while the central domain is more enriched with microtubules. Retrograde flow is powered in part by myosin II (25). To determine whether myosin II forces contribute to the wavy contour of microtubules in the growth cone, we determined whether treatment with blebbistatin, a pharmacological inhibitor of myosin II, can reduce the number of microtubules with wave-like folds in control growth cones and reverse the increase caused by depletion of DCX and DCLK. Control and DCX+DCLK-depleted neurons were re-plated and then stimulated to extend axons with laminin as described in Materials and Methods. After 1.5 h, after which the majority of the neurons had extended axons with large growth cones, the cultures were treated with 50 μM blebbistatin or DMSO, the vehicle for the drug, for 30 min. The cells were then fixed and stained for microtubules to assess the configuration of growth cone microtubules.

As expected, treatment with blebbistatin dramatically increased microtubule invasion into the peripheral domain of the growth cone (26,28), and this was true for both control and DCX+DCLK-depleted neurons (data not shown). Blebbistatin treatment of control neurons had an overall straightening effect on microtubules throughout the growth cone (Fig. 9A and B) and reduced the occurrence of microtubules with wave-like folds, although the change was not statistically significant (12 versus 9% for DMSO or blebbistatin-treated neurons, respectively, $P > 0.1$, χ^2-test) (Fig. 10). In DCX+-DCLK-depleted neurons, blebbistatin treatment reduced the tangled appearance of the microtubule array in the growth cone (Fig. 9C and D) and also reduced the occurrence of microtubules with wave-like folds to near control levels (Fig. 10); the difference in the frequency of microtubules with wave-like folds in DCX+DCLK-depleted neurons treated with blebbistatin versus DMSO (15 versus 26%, respectively) was statistically significant ($P < .01$, χ^2-test). These results support a role for DCX and DCLK in enabling growth cone microtubules to remain relatively straight when subjected to forces that would otherwise cause them to buckle.

Depletion of DCX+DCLK reduces the extent of microtubule invasion into filopodia

Under normal conditions, forces generated by myosin II function to antagonize microtubule invasion into the filopodia of the growth cone (27). This raises the possibility that depleting DCX and DCLK may impair the extension of microtubules into the growth cone periphery. We explored this possibility by quantifying microtubule invasion into growth cone filopodia of control and DCX+DCLK-depleted neurons using time-lapse imaging of EGFP-EB3 to visualize microtubule invasion. Neurons were co-transfected with EGFP-EB3 cDNA

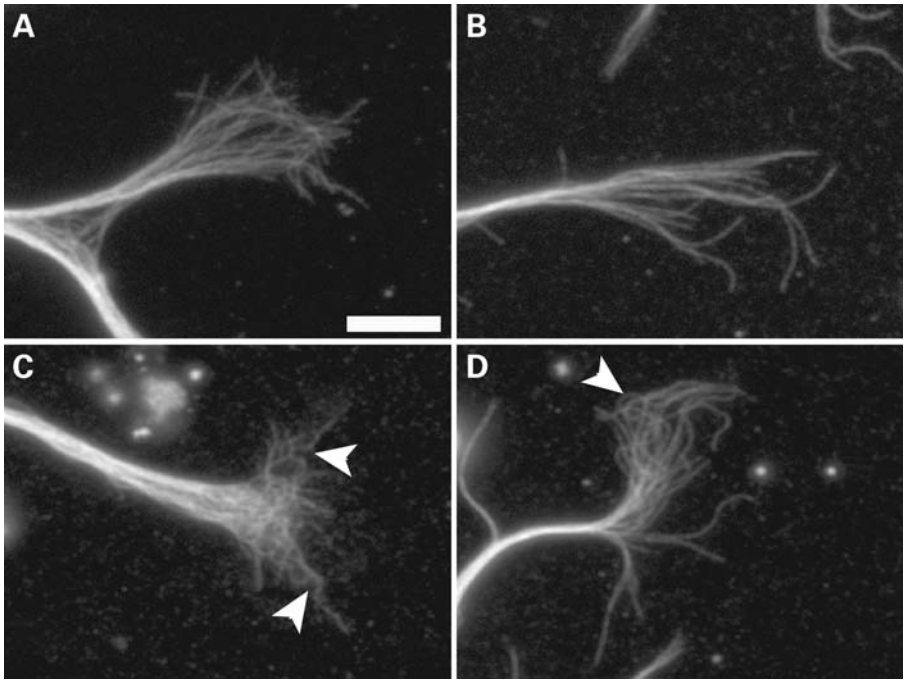

Figure 9. Inhibition of myosin-II with blebbistatin reduces the percentage of microtubules with wave-like folds in growth cones of neurons depleted of DCX and DCLK. (**A** and **B**) Control growth cones treated with DMSO or blebbistatin. Treatment with blebbistatin did not significantly decrease the levels of microtubules with wave-like folds in control growth cones. (**C**–**D**) Growth cones of DCX+DCLK siRNA neurons that were treated with DMSO or blebbistatin. Treatment with blebbistatin significantly decreases the number of microtubules with wave-like folds resulting from DCX+DCLK depletion. Scale bar = 6 μm.

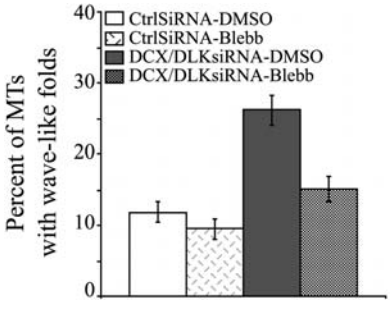

Figure 10. Quantitative analyses showing the effect of blebbistatin treatment on microtubules with wave-like folds. The graph shows the percentage of microtubules with wave-like folds in growth cones of control neurons and neurons depleted of DCX+DCLK after treatment with either DMSO or blebbistatin (Blebb). Combined knockdown of both DCX and DCLK significantly increased the frequency of microtubules with wave-like folds (from 12 to 26%, $P < 0.0001$, χ^2-test, based on analyses of 73 growth cones of control neurons treated with DMSO and 53 growth cones of DCX+DCLK-depleted neurons treated with DMSO). Treatment with blebbistatin reduced the percentage of microtubules with wave-like folds in control neurons, but this effect was not statistically significant ($P > 0.05$ χ^2-test, based on analyses of microtubules in 73 growth cones treated with control siRNA and DMSO and 72 growth cones treated with control siRNA and blebbistatin). Blebbistatin treatment of neurons depleted of DCX and DCLK significantly reduced the frequency of microtubules with wave-like folds (from 26 to 15%, $P < 0.01$, χ^2-test, based on analyses of 53 growth cones treated with DCX+DCLK siRNA and DMSO and 51 growth cones treated with DCX+DCLK siRNA and blebbistatin) MTs, microtubules.

and the relevant siRNAs, plated for 3 days and then re-plated and stimulated to extend axons by treatment with laminin (see Materials and Methods). Approximately 1–2 h after stimulation with laminin, 3 min time-lapse movie sequences were obtained of EGFP-EB3. We evaluated both the number of EB3 comets that entered the peripheral domain and the depth that comets extended into filopodia that were 2 or more microns in length. No significant differences were noted in the average length of filopodia between control and DCX+DCLK-depleted neurons. The average length of control filopodia was 5.57 ± 2.3 μm (mean ± SD, $n = 23$ filopodia), while filopodia of neurons depleted of DCX and DCLK were 4.98 ± 1.6 μm ($n = 38$) in length ($P > 0.1$, *t*-test). In addition, the duration of microtubule growth events, calculated as the duration of the EB3 comets, was comparable in growth cones of control and DCX+DCLK-depleted neurons [22.9 s ($n = 68$ comets) for control and 19.75 s ($n = 45$) for depleted ($P > 0.1$, *t*-test)]. The number of microtubules invading the peripheral domain of the growth cone, including both lamellipodia and filopodia per unit time, was comparable in control and depleted neurons. Specifically, based on 1 min video sequences of EGFP-EB3, the number of EB3 comets entering the peripheral domain of control and depleted growth cones per minute was 8.8 ± 5.92 (mean ± SD, $n = 10$ growth cones) and 9.25 ± 4.89 ($n = 8$ growth cones), respectively. These values are statistically indistinguishable from each other ($P > 0.1$, *t*-test). To evaluate the depth of microtubule invasion into filopodia, each analyzed filopodium was segmented into three equal fractions of its total length consisting of a proximal, middle or distal region relative to the growth cone. We tracked the EGFP-EB3 comets for 1 min and determined where within each filopodium the comets disappeared, defining this as the maximum extent of microtubule invasion. We found that the relative depth that comets invaded growth cone filopodia was

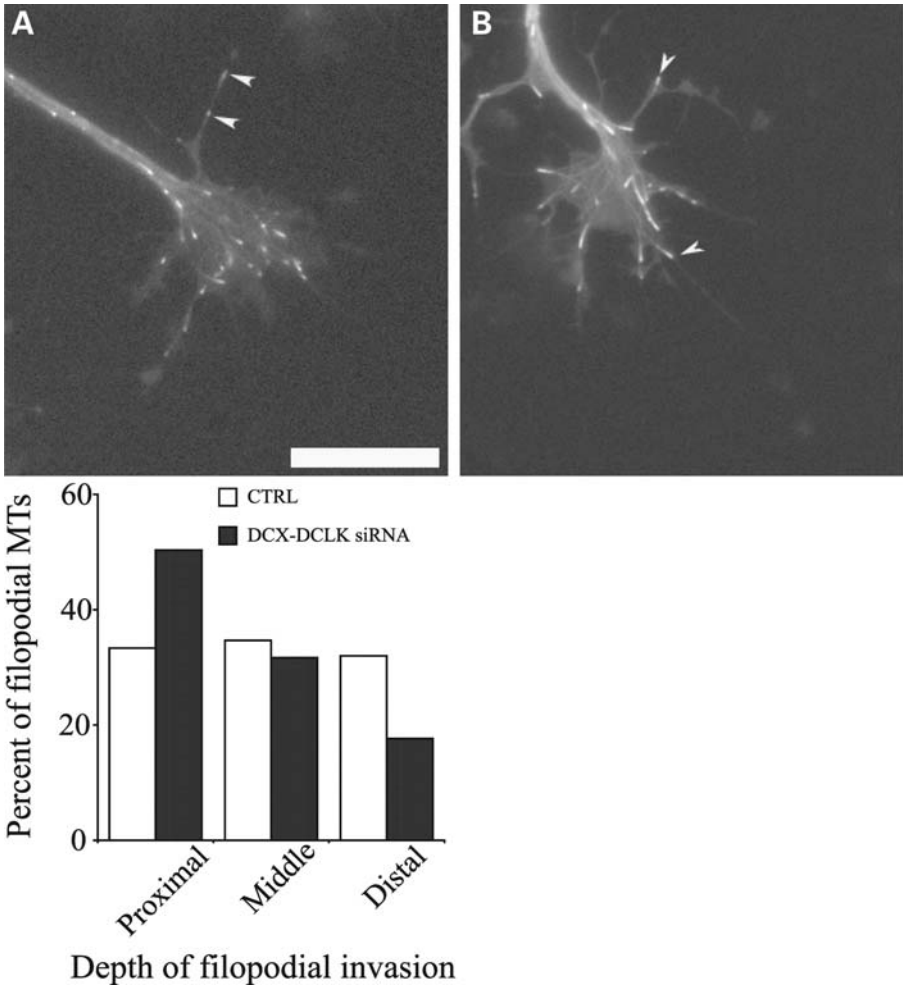

Figure 11. Depletion of DCX and DCLK reduces the depth of microtubule invasion into growth cone filopodia. We performed time-lapse imaging of EGFP-EB3 to evaluate microtubule invasion into growth cone filopodia. Neurons were co-transfected with EGFP-EB3 cDNA and either control siRNA or DCX+DCLK siRNA, cultured for 3 days and then re-plated in preparation for time-lapse imaging of EB3 comets (see Materials and Methods for details). (**A** and **B**) Still-frames from time-lapse video sequences of a control and a DCX+DCLK-depleted growth cone. Numerous EB3 comets are apparent in the growth cones, some of which have entered filopodia (white arrowheads). To quantify the depth of comet invasion into filopodia, we used the time-lapse sequences to track and record the most distal portion of the filopodia reached by the EGFP-EB3 comet. The quantitative analyses, based on analyses of 13 control and 13 depleted growth cones, are depicted in the graph. On average, the relative distance that microtubules invaded filopodia was significantly less in depleted neurons compared with control neurons ($P < 0.0001$, χ^2-test). Scale bar = 6 μm.

significantly less in DCX+DCLK-depleted cells compared with controls (Fig. 11). Specifically, in control neurons, comets extended variable distances into filopodia before disappearing, with approximately one-third of the comets disappearing within the proximal region, one-third disappearing in the middle region and one-third disappearing in the distal region. In contrast, in cells depleted of DCX and DCLK, 50% of the comets entering filopodia disappeared within the proximal region, whereas fewer than 20% reached into the distal region. This difference in filopodial invasion was statistically highly significant ($P < 0.0001$, χ^2-test).

DCX+DCLK depletion alters the behavior of growth cones at substrate borders

A key function of growth cones is to detect guidance cues in the environment and initiate changes in growth cone structure and motility to steer the axon in the appropriate direction. These responses are mediated by the growth cone cytoskeleton (reviewed in 29–31). One of the key cytoskeletal events required for successful growth cone steering is the invasion of selected filopodia by microtubules. This stabilizes a filopodium so that it can undergo continued elongation and ultimately convert into new axon oriented in the proper direction (32–34). Because depletion of both DCX and DCLK impairs microtubule invasion into filopodia (see above), it seems reasonable that this may also impair growth cone steering. We have explored this possibility using a substrate border assay. In such assays, a patterned substrate is created using two different substrate components, one more preferred for growth than the other. Control and experimental neurons are plated on one substrate and allowed to extend axons that eventually encounter the border with the other substrate. It is then determined whether the experimental manipulation changes the axonal

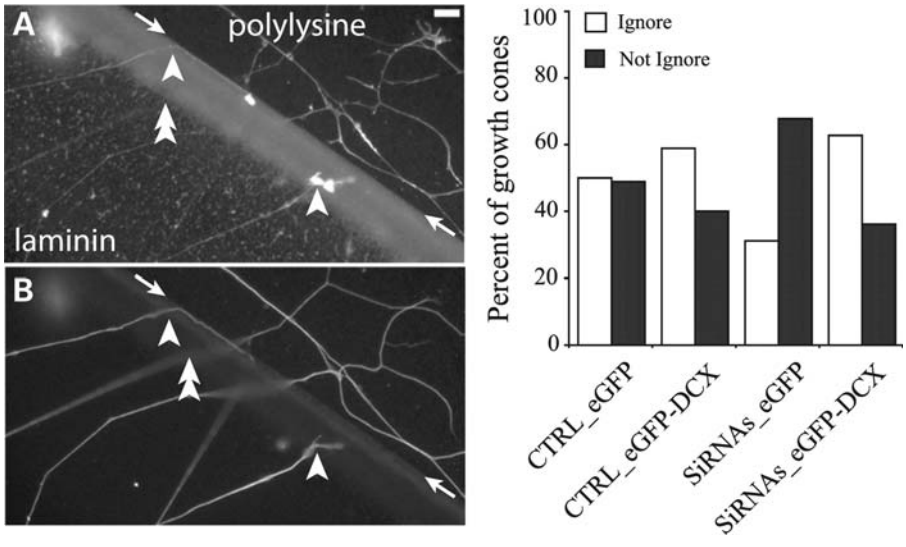

Figure 12. Behavior of growth cones at a substrate border of neurons depleted of DCX and DCLK. Neurons were co-transfected with control siRNA (CTRL) or DCX+DCLK siRNA (siRNAs) and either cDNAs to EGFP alone or EGFP tagged DCX, plated on a poly-D-lysine substrate for 3 days and then re-plated on a discrete area of laminin on the surface of a uniform poly-D-lysine substrate as described in the Materials and Methods section. Upon reaching the border between the laminin and poly-D-lysine, the growth cones of axons originating on the laminin side can either cross the border ('ignore) or remain on the laminin side ('not ignore'). After fixation, the neurons were stained to reveal laminin, actin filaments and tubulin as described in Materials and Methods. (**A**) An image showing both laminin and actin staining, whereas (**B**) shows the same field stained for tubulin (the scale bar = 9 μm). The border between the laminin and poly-D-lysine is indicated by the arrows; we note that the staining for laminin was somewhat greater at the border than at regions internal to the border. Within the images are examples of axons that either ignored (double arrowhead) or did not ignore (single arrowhead) the border. The focal plane of axons commonly changed as they approached the border. We counted axons that ignored or did not ignore the border under the various conditions and the results are shown in the graph (a minimum of 120 axons were counted for each condition). In cultures of control neurons, ~50% of the axons either ignored or did not ignore the border. Overexpression of human DCX increased the percentage of axons ignoring the border, although the difference was not statistically significant ($P > 0.05$, χ^2-test). Depletion of both DCX and DCLK reduced the percentage of axons that ignored the border compared with controls (from ~50 to ~30%, $P < 0.0001$, χ^2-test, CTRL-EGFP versus DCX+DCLK siRNA with EGFP). In neurons treated with DCX+DCLK siRNAs, overexpression of human DCX reversed the effects of siRNA treatment alone such that the percentage of growth cones ignoring the borders resembled that in control neurons over-expressing EGFP-DCX.

growth behavior at the border (16). Two general behaviors are possible in these types of experiments; either the growth cone will steer the axon to remain on the starting substrate or the growth cone will ignore the border and extend onto the other substrate. Given that depletion of both DCX and DCLK reduces the extent of microtubule invasion into filopodia, we expected that such depleted growth cones would be less likely than control growth cones to ignore the border to grow onto the other substrate. To maximize our chances of detecting such an effect, we designed a border assay using poly-D-lysine and laminin substrates that would provide a relatively modest challenge to control neurons (see Materials and Methods). Under the conditions of this assay, ~50% of control growth cones that encountered the border between laminin and poly-D-lysine ignored the border and grew onto the poly-D-lysine substrate, while the remaining growth cones stayed on the laminin substrate (Fig. 12). Under these same conditions, growth cones of neurons depleted of DCX and DCLK had a reduced ability to ignore this challenge and thus ~70% remained on the laminin side of the border. This impairment of DCX+DCLK depletion was significantly rescued back to control level by overexpressing ectopic DCX (Fig. 12).

DISCUSSION

We have described a novel activity for DCX and DCLK that is manifested in the relative straightness of growth cone microtubules. Under normal conditions, most microtubules extending into the lamellar regions of the growth cone have a gently curved contour, while a relatively smaller proportion displays one or more wave-like folds along their length. Depletion of DCX+DCLK dramatically increases the occurrence of these wave-like folds, resulting in a tangled appearance of the microtubule array. In contrast, overexpression of DCX dramatically reduces the appearance of wave-like folds and notably straightens the microtubules. Furthermore, expression of ectopic DCX is sufficient to rescue the phenotype caused by depletion of endogenous DCX+DCLK, suggesting that the observed effect of the double knockdown is specifically due to loss of microtubule-binding activity as opposed to other possible functions of the kinase domain of DCLK. The straightening function of DCX and DCLK appears to be either unique to these proteins or accentuated compared with other microtubule-associated proteins, as we observed no enhancement in microtubule bending when MAP1B was depleted.

Analysis of the distribution of DCX along individual microtubules in the growth cone fortifies the case that these proteins regulate microtubule straightness. Microtubules that exhibit a straight or moderately curved contour displayed relatively continuous DCX along their length, whereas regions of microtubules with wave-like folds or just prominent bends were relatively deficient in DCX. Interestingly, previous studies indicated that tau is enriched on regions of neuronal microtubules with prominent bends (35), which is precisely the inverse of the distribution of DCX. We previously reported

that tau and DCX do, in fact, have inverse distributions on growth cone microtubules (8). Moreover, we reported that when neurons are depleted of DCX, tau redistributes to associate with regions of microtubules that would otherwise be rich in DCX. These observations raise the possibility that it is actually the balance between tau and DCX family proteins that determine the straightness of the microtubule. Perhaps, tau renders the microtubule more flexible, and its displacement by DCX family proteins results in a straighter microtubule because of the lack of tau. Alternatively, perhaps either one can contribute to microtubule straightness, but the DCX family proteins are far better at carrying out this function than tau. The latter possibility seems more likely, given previous studies indicating that binding of microtubule-associated proteins in the tau family to a microtubule increases its flexural rigidity (36). Future studies on the relationship between these proteins will be of great interest, particularly given that tau plays key roles in neurodegenerative disorders while the DCX proteins play key roles in neurodevelopmental disorders.

We are using the term 'straighten' rather than 'stiffen' to be cautious, but presumably the microtubules are straighter because they are more resistant to bending, which would make them stiffer as well. The simplest explanation for this would be that the binding of DCX and DCLK to the microtubule directly confers stiffness to the polymer. In support of this, the microtubule-binding site of DCX and DCLK lies between the protofilaments, which is thought to be the weakest point in the microtubule wall (13). In this view, DCX is postulated to 'staple' protofilaments together and also act at the tubulin junctions along the protofilaments to prevent microtubules from folding (13).

The bending of microtubules into wave-like folds gives the appearance of microtubules that are buckling in response to externally applied forces. Best known of these forces is the retrograde flow of actin filaments in the peripheral domain, driven by myosin II (24,37). Recent studies indicate that cytoplasmic dynein imposes an antagonistic force on the microtubules that drive them from the central domain into the peripheral domain, against the retrograde actin flow (28,38). Forces generated by certain kinesins, namely kinesins 5 and 12, impose forces that antagonize dynein's forces, and are hence additive with the myosin II forces (15,16). The forces of myosin II push the majority of the microtubule mass into the central domain, but a small number of microtubules are able to overcome these forces and extend in a relatively straight fashion to invade filopodia. We found that inhibition of myosin II significantly reduced the number of microtubules with wave-like folds and the consequent tangling effect of the microtubule array in the growth cones of neurons depleted of DCX and DCLK. However, the occurrence of such curvatures was not entirely abolished, suggesting that other factors, such as the forces generated by kinesins 5 and 12, contribute to the bending and tangling of microtubules.

Tangling of growth cone microtubules can also result from depletion of cytoplasmic dynein or Lis1 (28,38,39). Lis1 has been reported to facilitate the ability of dynein to generate forces on microtubules (38,40), and the same could be true of DCX, given the similar phenotypes resulting from mutations to each of these two proteins (1). Thus, another potential interpretation of our observations is that the DCX family of proteins straightens microtubules by promoting the forces generated on them by cytoplasmic dynein. In this view, depleting DCX and DCLK would reduce the anterograde forces generated on microtubules by dynein, and thereby result in greater tangling. If DCX family members enhance the ability of growth cone microtubules to resist the retrogradely oriented forces, then microtubule invasion into the peripheral domain should be impaired by their depletion. Indeed, we found the depth of filopodial invasion by microtubules to be reduced in DCX+DCLK-depleted cells. Microtubules of control neurons were uniformly distributed within the proximal to distal region of filopodia, while those of DCX+-DCLK-depleted neurons were mainly restricted to the proximal region.

Filopodia play crucial roles during axonal guidance where they detect guidance signals that lead to the polarization of the growth cone in the direction of the cue (41,42). This requires the advance of microtubules from the central domain into the peripheral domain, thereby providing the architectural support and transport substrate necessary for continued axonal extension (32–34). Altered invasion of microtubules into the peripheral domain can thereby impact growth cone steering. For example, inhibition of myosin II or kinesins 5 or 12 leads to robust and indiscriminate invasion of microtubules throughout the peripheral domain, and failure of growth cones to turn at substrate borders (15,16,43). Here, we used a modified border assay to determine whether the effect of DCX+DCLK depletion on microtubule invasion of filopodia was also associated with altered behavior at substrate borders. In this border assay, in which ~50% of control growth cones ignored the border and 50% remained on laminin, a much greater percentage of DCX+DCLK-depleted growth cones failed to cross the border and instead remained on the laminin. This effect was reversed by overexpressing DCX, which enhanced microtubule extension into the distal reaches of the growth cone. Thus, the altered behavior of DCX+DCLK-depleted growth cones in the border assay results at least in part from the impaired ability of microtubules to invade growth cone filopodia.

The implications of our observations on the impact of DCX+DCLK depletion on microtubules may extend beyond growth cone steering. There are many other processes that could be affected by the abnormal tangling of the microtubules in the growth cone that could impact axonal growth. While the tangling had only a modest effect on the capacity of depleted axons to grow, we note that rat sympathetic neurons grow very vigorously in culture and there are very few manipulations that impair their growth. Thus, the relatively modest effect we observed is noteworthy. The various cellular processes that support axonal growth depend on the appropriate configuration of the microtubule cytoskeleton. For example, microtubules need to align and bundle in the neck region of the growth cone in a phase of axonal growth known as consolidation (44). In terms of bundling, several papers have documented that over-expression of DCX in non-neuronal cells increased microtubule bundling (45,46), while knock down of DCX in neurons has been reported to result in reduced bundling (47). However, our present work unequivocally shows that over-expression of DCX did not result in

microtubule bundling in the growth cones of cultured sympathetic neurons. Similarly, microtubule bundling was not detectably enhanced by over-expression of DCLK in cultured cortical neurons (48). A potentially important function of the DCX family of proteins may be to combat the tendency of growth cone microtubules to tangle by promoting their straightness to support its function in axonal transport. For example, organelles need to directionally advance along microtubules as they reach the distal region of the axon and also as they transit back into the axon from the growth cone to move retrogradely back to the cell body. Short microtubules must also appropriately transit from the central domain to the more lamellar regions of the peripheral domain (49) and such transport could lose directionality if the microtubule array is abnormally tangled. Thus, flaws in DCX and DCLK could lead to developmental abnormalities not only by reducing the capacity of microtubules to invade filopodia, but also by allowing the microtubules to become abnormally tangled elsewhere in the growth cone.

MATERIALS AND METHODS

Materials

Culture dishes in which glass cover slips had been fixed to the bottom over a hole of 14 mm were obtained from Matek. Culture media and relevant supplements were obtained from Invitrogen, except for BSA, which was obtained from Calbiochem, and fetal bovine serum, which was obtained from HyClone Laboratories. Other reagents were obtained from Sigma-Aldrich, unless otherwise indicated.

Cell culture

Primary cultures of newborn rat sympathetic neurons were generated as previously described (8). Briefly, sympathetic neurons were dissociated from the superior cervical ganglia of newborn-1-day-old rat pups using sequential treatments with collagenase and trypsin, followed by trituration as previously described (50). Dissociated neurons were transfected with various siRNA reagents, and in some experiments together with DNA constructs as described below and then plated at high density on plastic culture dishes coated with 0.5 mg/ml poly-D-lysine in L15 media with 10% fetal calf serum and 100 ng/ml NGF. The plating medium was changed from L15 to serum-free N2 medium the day after plating to delay the proliferation of non-neuronal cells. After 3 days, the cells were re-dissociated by treatment with 0.25% trypsin/EDTA for 3–5 min followed by gentle trituration and re-plated in the Matek dishes described above. The glass surface in these dishes had been coated with 0.1 mg/ml poly-D-lysine. The medium consisted of serum-free N2 with the standard N2 supplements and NGF. Under these conditions, neurons plated at medium to low density attach to the substrate but fail to extend axons. The following day, the cultures were treated with 25 μg/ml laminin in the culture medium to stimulate rapid axonal outgrowth (17–19), and used for experiments within 2–3 h. As described below, cells were re-plated after 3 days because this time was required for the siRNA treatment to effectively deplete DCX and DCLK.

RNA interference

Dissociated cells from the superior cervical ganglia of postnatal rat pups (days 0–1) were nucleofected with the appropriate siRNAs, as previously described (8) to deplete DCX and DCLK. Four different siRNA duplexes were designed against different regions of the DCX and DCLK sequences using Sigma's custom SMARTpool siRNA service (rat cytoplasmic DCX, accession number NM_053379, rat cytoplasmic DCLK 1, accession number NM_053343). The non-specific duplex III from Sigma was used as control. siRNA was dissolved to 400 μM, aliquoted and stored at −20°C. siRNA concentration at nucleofection was 18 μM.

Overexpression studies

Plasmids containing EGFP-tagged human DCX cDNA, EGFP-EB3 cDNA or control cDNA consisting of EGFP alone were introduced into the cells together with the siRNAs by nucleofection using our standard procedures (8,15,28). The DCX construct was provided by Dr Joseph Gleeson, while the EB3 construct was provided by Dr Niels Galjart (20).

Blebbistatin studies

On the day after re-plating, 25 μg/ml of laminin was added to the medium for 1.5 h to stimulate rapid axonal growth. Once that time had elapsed, 50 μM of blebbistatin was added to the culture medium for 30 min after which the cells were fixed as described below.

Immunofluorescence procedures

We generally used the combined fixation/extraction and staining procedure as previously described (8), although staining for DCLK required fixation in cold (−20°C) methanol for 6 min followed by rehydration in phosphate buffered saline. Microtubules were revealed using a mouse monoclonal antibody against alpha-tubulin [DM1 alpha, provided by Dr V. Gelfand, University of Illinois (51)]. To reveal DCX, we used a rabbit polyclonal antibody raised against the C-terminus of human DCX, which was purchased from Abcam. DCLK was revealed using a goat polyclonal raised against the C-terminus of human DCLK, which we purchased from Santa Cruz Biotechnology. Each of these antibodies was used at a final concentration of 4 μg/ml. Fluorescently labeled secondary antibodies were obtained from Jackson Immunoresearch (West Grove, PA, USA). Rhodamine phalloidin was used to reveal actin filaments (8). In experiments overexpressing EGFP-DCX, cells were fixed without extraction and then stained for GFP using primary antibodies obtained from Abcam and Cy2-labeled secondary antibodies obtained from Jackson Immunoresearch.

Imaging and analysis

Imaging of fixed or live cells was performed with a Zeiss Axiovert 200M to which was interfaced a Cooke sensicam cooled CCD camera. The camera, shutter and motorized microscope components were controlled using iVision software (Biovision Technologies, Exton, PA, USA). Filter sets optimized for multiple labeling analyses using Cy2, Rhodamine Red-X and Cy5 were obtained from Chroma (Rockingham, VT, USA). Images of fixed cells were acquired using the full usable area of the CCD chip, which measured 1376 × 1024 pixels and stored in full 12-bit format for processing and analysis. High-resolution images of growth cone microtubules were obtained with the 100×/1.3 Plan-Neofluar oil objective. To avoid selection bias in these analyses, we predetermined a minimum number of growth cones to analyze, usually 50–100, and took images of every neuron encountered up to the pre-determined number.

Live-cell imaging of EGFP-EB3

Time-lapse images were obtained of EGFP-EB3 to visualize growing microtubules in the growth cone. Imaging was performed with a 100×/1.3 Plan Neofluar oil objective. Sequences of 3 min in duration were recorded using 500 ms exposures and 1 s intervals between frames. All experiments included only low-to-moderate expressers, as high expression of EB3 can alter microtubule dynamics. After time-lapse imaging, the cultures were fixed and stained for DCX and DCLK to confirm the extent of depletion in the general population. We were unable to specifically evaluate the level of depletion in each cell that was imaged because the ×100 objective cannot be used with the gridded dishes that we use to track individual cells. However, our evaluation of the population indicated that over 85% of the cells showed marked diminution of the targeted proteins.

Image processing was performed with various tools in iVision or Oncor image. Images were imported into Adobe Photoshop and Adobe illustrator to prepare figures for presentation (version CS3 extended); unless otherwise indicated, linear methods were used to enhance image brightness and contrast for presentation.

Quantitative analysis of the effects of DCX and DCLK depletion or DCX overexpression on the contour of growth cone microtubules

To pursue initial qualitative observations suggesting that depletion of DCX and DCLK resulted in more bending of microtubules in the growth cone and our later observation that overexpression of DCX has the opposite effect, we wished to develop an unbiased means for quantifying these effects. We focused our attention on individual microtubules that displayed multiple bends over a relatively short distance along their length, which created a configuration that we termed wave-like folds. We scored individual microtubules in the growth cone that could clearly be traced from their distal (plus) end for at least 5 μm as either positive or negative for wave-like folds. To be scored positive for the presence of wave-like folds, a microtubule would have to display at least four consecutive and prominent bends within a maximal distance of 5 μm (Fig. 3).

Analyses of wave like-folds were conducted on fixed cells immunostained for alpha-tubulin, and also on living cells using time-lapse imaging of EGFP-EB3 comets. For analyses on fixed cells, for each growth cone, we counted the total number of microtubules that could be clearly traced to their plus ends. Then, we determined the number of these that had one or more wave-like folds along their length using the criteria specified above. The number of microtubules with wave-like folds was then expressed as a percent of the total number of microtubules evaluated. To quantify microtubules with wave-like folds using live-cell imaging, we approximated the region of the peripheral domain in each growth cone and then counted the total number of microtubules (visualized with EGFP-EB3) that appeared in that region within two predetermined 30 s segments of the video records (specifically within frames 0–30 and frames 90–120 of the 3 min sequence). The number with folds was then normalized to the total number of microtubules evaluated, and the χ^2-test was used to compare the results obtained in control versus experimental groups.

Modified substrate border assay

In the previous work, we used border assays to examine the behavior of growth cones as they encounter a border between substrates containing laminin or poly-D-lysine. In adapting these assays for our earlier studies, we optimized conditions so that very few control axons would cross from the laminin side of the border onto the poly-D-lysine side (16). This was so that we could test the role of certain proteins in enabling the axon to turn at the border. Failure to turn manifests as a greater number of axons crossing the border. Here, we modified the assay so that it would permit far more crossing, in order to test the prediction that depletion of DCX and DCLK would actually reduce the amount of crossing. The principal change to the procedure involved plating newly dissociated neurons on poly-D-lysine instead of laminin. Then, 3 days later, the cells were re-plated and challenged with laminin-poly-D-lysine borders (see below). By plating initially on poly-D-lysine instead of laminin, we prevent priming of the neurons to laminin that is potentially induced by their introduction to this neurotrophic factor both during plating and re-plating. By not sensitizing the neurons to laminin during the initial plating, we reasoned that when subsequently challenged with a border between laminin and poly-D-lysine, they would be much more likely to ignore the border and grow from laminin onto poly-D-lysine. As described in the Results section, this is exactly what happened.

In our modified assay, freshly dissociated neurons were subjected to nucleofection to introduce siRNAs or siRNAs+-EGFP-DCX or control cDNA, and then they were plated onto a poly-D-lysine substrate as described above. The neurons were then re-plated on specially coated dishes 3 days after the initial plating. These dishes had been prepared by coating them overnight with poly-D-lysine, rinsing them extensively with distilled water and then allowing them to air-dry for at least 1 h. Subsequently, a 50 μl drop of 25 μg/ml laminin was added to the center of the dish and left undisturbed for 2 h.

This created a circle of laminin of ~7 mm in diameter. Dissociated cells were plated onto the laminin area in 45 μl of the supplemented N2 medium; 2 h later, after the cells had attached to the laminin, 1.5 ml of the supplemented N2 medium was added to the dishes. The cells were fixed 48–60 h later using the fix-extraction procedures described above. At this time, many axons had reached and reacted to the border. For analysis, the cultures were stained with antibodies to laminin to reveal the laminin substrate and its border with the poly-D-lysine-only substrate and for actin filaments using Rhodamine-phalloidin. In addition, the cells were also stained for tubulin or, in experiments in which cells were also transfected with DNA constructs for EGFP fusion proteins, the cells were stained for EGFP to identify expressing neurons. To quantify growth cone behavior at the borders, we examined the entire border (~22 mm perimeter) between laminin and poly-D-lysine in each dish, and every axon at the border was categorized as ignoring if it grew from the laminin onto the poly-D-lysine or not-ignoring if it remained on the laminin. In experiments in which the neurons were also transfected with EGFP constructs, the axons at the borders were also scored for the presence or absence of staining for GFP.

ACKNOWLEDGEMENTS

We thank Joseph Gleeson for DNA constructs.

Conflict of Interest statement. None declared.

FUNDING

This work was supported by grants from the National Institutes of Health (R01 NS28785) and the National Science Foundation (0841245) to P.W.B.

REFERENCES

1. Portes, V.d., Pinard, J.M., Billuart, P., Vinet, M.C., Koulakoff, A., Carrié, A., Gelot, A., Dupuis, E., Motte, J., Berwald-Netter, Y. *et al.* (1998) A novel CNS gene required for neuronal migration and involved in x-linked subcortical laminar heterotopia and lissencephaly syndrome. *Cell*, **9**, 51–61.
2. Taylor, K.R., Holzer, A.K., Bazan, J.F., Walsh, C.A. and Gleeson, J.G. (2000) Patient mutations in doublecortin define a repeated tubulin-binding domain. *J. Biol. Chem.*, **275**, 34442–34450.
3. Deuel, T.A.S., Liu, J.S., Corbo, J.C., Yoo, S.-Y., Rorke-Adams, L.B. and Walsh, C.A. (2006) Genetic interactions between doublecortin and doublecortin-like kinase in neuronal migration and axon outgrowth. *Neuron*, **49**, 41–53.
4. Koizumi, H., Tanaka, T. and Gleeson, J.G. (2006) doublecortin-like kinase functions with doublecortin to mediate fiber tract decussation and neuronal migration. *Neuron*, **49**, 55–66.
5. Friocourt, G., Koulakoff, A., Chafey, P., Boucher, D., Fauchereau, F., Chelly, J. and Francis, F. (2003) Doublecortin functions at the extremities of growing neuronal processes. *Cereb. Cortex*, **13**, 620–626.
6. Schaar, B.T., Kinoshita, K. and McConnell, S.K. (2004) Doublecortin microtubule affinity is regulated by a balance of kinase and phosphatase activity at the leading edge of migrating neurons. *Neuron*, **41**, 203–213.
7. Gdalyahu, A., Ghosh, I., Levy, T., Sapir, T., Sapoznik, S., Fishler, Y., Azoulai, D. and Reiner, O. (2004) DCX, a new mediator of the JNK pathway. *EMBO J.*, **23**, 823–832.
8. Tint, I., Jean, D., Baas, P.W. and Black, M.M. (2009) Doublecortin associates with microtubules preferentially in regions of the axon displaying actin-rich protrusive structures. *J. Neurol.*, **29**, 10995–11010.
9. Burgess, H.A. and Reiner, O. (2000) Doublecortin-like kinase is associated with microtubules in neuronal growth cones. *Mol. Cell. Neurol.*, **16**, 529–541.
10. Geraldo, S. and Gordon-Weeks, P.R. (2009) Cytoskeletal dynamics in growth-cone steering. *J. Cell Sci.*, **122**, 3595–3604.
11. Tsukada, M., Prokscha, A., Oldekamp, J. and Eichele, G. (2003) Identification of neurabin II as a novel doublecortin interacting protein. *Mech. Dev.*, **120**, 1033–1043.
12. Tsukada, M., Prokscha, A., Ungewickell, E. and Eichele, G. (2005) Doublecortin association with actin filaments is regulated by neurabin II. *J. Biol. Chem.*, **280**, 11361–11368.
13. Moores, C.A., Perderiset, M., Francis, F., Chelly, J., Houdusse, A. and Milligan, R.A. (2004) Mechanism of microtubule stabilization by doublecortin. *Mol. Cell*, **14**, 833–839.
14. Corbo, J.C., Deuel, T.A., Long, J.M., LaPorte, P., Tsai, E., Wynshaw-Boris, A. and Walsh, C.A. (2002) Doublecortin is required in mice for lamination of the hippocampus but not the neocortex. *J. Neurosci.*, **22**, 7548–7557.
15. Nadar, V.C., Ketschek, A., Myers, K.A., Gallo, G. and Baas, P.W. (2008) Kinesin-5 is essential for growth-cone turning. *Curr. Biol.*, **18**, 1972–1977.
16. Liu, M., Nadar, V.C., Kozielski, F., Kozlowska, M., Yu, W. and Baas, P.W. (2010) Kinesin-12, a mitotic microtubule-associated motor protein, impacts axonal growth, navigation, and branching. *J. Neurosci.*, **30**, 14896–14906.
17. Rivas, R.J., Burmeister, D.W. and Goldberg, D.J. (1992) Rapid effects of laminin on the growth cone. *Neuron*, **8**, 107–115.
18. Slaughter, T., Wang, J. and Black, M.M. (1997) Microtubule transport from the cell body into the axons of growing neurons. *J. Neurol.*, **17**, 5807–5819.
19. Yu, W., Ling, C. and Baas, P. (2001) Microtubule reconfiguration during axogenesis. *J. Neurol.*, **30**, 861–875.
20. Stepanova, T., Slemmer, J., Hoogenraad, C.C., Lansbergen, G., Dortland, B., De Zeeuw, C.I., Grosveld, F., van Cappellen, G., Akhmanova, A. and Galjart, N. (2003) Visualization of microtubule growth in cultured neurons via the use of EB3-GFP. (End-binding protein 3-green fluorescent protein). *J. Neurosci.*, **23**, 2655–2664.
21. Black, M.M., Slaughter, T. and Fischer, I. (1994) Microtubules-associated protein 1b. (MAP1b) is concentrated in the distal region of growing axons. *J. Neurosci.*, **2**, 857–870.
22. Qiang, L., Yu, W., Andreadis, A., Luo, M. and Baas, P.W. (2006) Tau protects microtubules in the axon from severing by katanin. *J. Neurosci.*, **26**, 3120–3129.
23. Takei, Y., Teng, J., Harada, A. and Hirokawa, N. (2000) Defects in axonal elongation and neuronal migration in mice with disrupted tau and map1b genes. *J. Cell Biol.*, **150**, 989–1000.
24. Gonzalez-Billault, C., Avila, J. and Cáceres, A. (2001) Evidence for the role of MAP1B in axon formation. *Mol. Biol. Cell*, **12**, 2087–2098.
25. Lin, C.H., Espreafico, E.M., Mooseker, M.S. and Forscher, P. (1996) Myosin drives retrograde F-actin flow in neuronal growth cones. *Neuron*, **16**, 769–782.
26. Brown, M.E. and Bridgman, P.C. (2003) Retrograde flow rate is increased in growth cones from myosin IIB knockout mice. *J. Cell Sci.*, **116**, 1087–1094.
27. Schaefer, A.W., Kabir, N. and Forscher, P. (2002) Filopodia and actin arcs guide the assembly and transport of two populations of microtubules with unique dynamic parameters in neuronal growth cones. *J. Cell Biol.*, **158**, 139–152.
28. Myers, K.A., Tint, I., Nadar, C.V., He, Y., Black, M.M. and Baas, P.W. (2006) Antagonistic forces generated by cytoplasmic dynein and myosin-II during growth cone turning and axonal retraction. *Traffic*, **7**, 1333–1351.
29. Bentley, D. and O'Connor, T.P. (1994) Cytoskeletal events in growth cone steering. *Curr. Opin. Neurobiol.*, **4**, 43–48.
30. Letourneau, P.C. (1996) The cytoskeleton in nerve growth cone motility and axonal pathfinding. *Perspect. Dev. Neurobiol.*, **4**, 111–123.
31. Kalil, K., Szebenyi, G. and Dent, E.W. (2000) Common mechanisms underlying growth cone guidance and axon branching. *J. Neurobiol.*, **44**, 145–158.
32. Sabry, J.H., O'Connor, T.P., Evans, L., Toroian-Raymond, A., Kirschner, M. and Bentley, D. (1991) Microtubule behavior during guidance of pioneer neuron growth cones in situ. *J. Cell Biol.*, **115**, 381–395.

33. Tanaka, E., Ho, T. and Kirschner, M.W. (1995) The role of microtubule dynamics in growth cone motility and axonal growth. *J. Cell Biol.*, **128**, 139–155.
34. Williamson, T., Gordon-Weeks, P.R., Schachner, M. and Taylor, J. (1996) Microtubule reorganization is obligatory for growth cone turning. *Proc. Natl Acad. Sci. USA*, **93**, 15221–15226.
35. Samsonov, A., Yu, J.-Z., Rasenick, M. and Popov, S.V. (2004) Tau interaction with microtubules in vivo. *J. Cell Sci.*, **117**, 6129–6141.
36. Felgner, H., Frank, R., Biernat, J., Mandelkow, E.M., Ludin, B., Matus, A. and Schliwa, M. (1997) Domains of neuronal microtubule-associated proteins and flexural rigidity of microtubules. *J. Cell Biol.*, **138**, 1067–1075.
37. Lin, C.H., Espreafico, E.M., Mooseker, M.S. and Forscher, P. (1997) Myosin drives retrograde F-actin flow in neuronal growth cones. *Biol. Bull,*, **192**, 183–185.
38. Grabham, P.W., Seale, G.E., Bennecib, M., Goldberg, D.J. and Vallee, R.B. (2007) Cytoplasmic dynein and LIS1 are required for microtubule advance during growth cone remodeling and fast axonal outgrowth. *J. Neurosci.*, **27**, 5823–5834.
39. Ahmad, F.J., He, Y., Myers, K.A., Hasaka, T.P., Francis, F., Black, M.M. and Baas, P.W. (2006) Effects of dynactin disruption and dynein depletion on axonal microtubules. *Traffic*, **7**, 524–537.
40. Tanaka, T., Serneo, F.F., Higgins, C., Gambello, M.J., Wynshaw-Boris, A. and Gleeson, J.G. (2004) Lis1 and doublecortin function with dynein to mediate coupling of the nucleus to the centrosome in neuronal migration. *J. Cell Biol.*, **165**, 709–721.
41. O'Connor, T.P. and Bentley, D. (1993) Accumulation of actin in subsets of pioneer growth cone filopodia in response to neural and epithelial guidance cues in situ. *J. Cell Biol.*, **123**, 935–948.
42. Gallo, G. and Letourneau, P.C. (2004) Regulation of growth cone actin filaments by guidance cues. *J. Neurobiol.*, **58**, 92–102.
43. Turney, S.G. and Bridgman, P.C. (2005) Laminin stimulates and guides axonal outgrowth via growth cone myosin II activity. *Nat. Neurosci.*, **8**, 717–719.
44. Dent, E.W. and Gertler, F.B. (2003) Cytoskeletal dynamics and transport in growth cone motility and axon guidance. *Neuron*, **40**, 209–227.
45. Horesh, D., Sapir, T., Francis, F., Wolf, S.G., Caspi, M., Elbaum, M., CHelly, J. and Reiner, O. (1999) Doublecortin, a stabilizer of microtubules. *Hum. Mol. Genet.*, **8**, 1599–1610.
46. Kim, M.H., Cierpicki, T., Derewenda, U., Krowarsch, D., Feng, Y., Devedjiev, Y., Dauter, Z., Walsh, C.A., Otlewski, J., Bushweller, J.H. and Derewenda, Z.S. (2003) The DCX-domain tandems of doublecortin and doublecortin-like kinase. *Nat. Struct. Biol.*, **10**, 324–333.
47. Bielas, S.L., Serneo, F.F., Chechlacz, M., Deerinck, T.J., Perkins, G.A., Allen, P.B., Ellisman, M.H. and Gleeson, J.G. (2007) Spinophilin facilitates dephosphorylation of doublecortin by PP1 to mediate microtubule bundling at the axonal wrist. *Cell*, **129**, 579–591.
48. Lin, P.T., Gleeson, J.G., Corbo, J.C., Flanagan, L. and Walsh, C.A. (2000) DCAMKL1 encodes a protein kinase with homology to doublecortin that regulates microtubule polymerization. *J. Neurosci.*, **20**, 9152–9161.
49. Dent, E.W., Callaway, J.L., Szebenyi, G., Baas, P.W. and Kalil, K. (1999) Reorganization and movement of microtubules in axonal growth cone and developing interstitial branches. *J. Neurosci.*, **19**, 8894–8908.
50. Brown, A., Slaughter, T. and Black, M.M. (1992) Newly assembled microtubules are concentrated in the proximal and distal regions of growing axons. *J. Cell Biol.*, **119**, 867–882.
51. Blose, S.H., Meltzer, D.I. and Feramisco, J.R. (1984) 10-nm filaments are induced to collapse in living cells microinjected with monoclonal and polyclonal antibodies against tubulin. *J. Cell Biol.*, **98**, 847–858